Acta Biochimica Polonica

Vol. 55 No. 1/2008, 151–160

on-line at: www.actabp.pl

Regular paper

A diadenosine 5′,5′′-P^1P^4 tetraphosphate (Ap_4A) hydrolase from *Arabidopsis thaliana* that is activated preferentially by Mn^{2+} ions

Blanka Szurmak[1], Aleksandra Wysłouch-Cieszyńska[1], Małgorzata Wszelaka-Rylik[2], Wojciech Bal[1, 3] and Marta Dobrzańska[1]✉

[1]*Institute of Biochemistry and Biophysics, Polish Academy of Sciences, Warszawa, Poland;* [2]*Institute of Physical Chemistry, Polish Academy of Sciences, Warszawa, Poland;* [3]*Central Institute for Labour Protection — National Research Institute, Warszawa, Poland*

Received: 25 November, 2007; revised: 21 February, 2008; accepted: 05 March, 2008
available on-line: 13 March, 2008

Asymmetrical diadenosine 5′,5′′-P^1P^4 tetraphosphate (Ap_4A) hydrolases are key enzymes controlling the *in vivo* concentration of Ap_4A — an important signaling molecule involved in regulation of DNA replication and repair, signaling in stress response and apoptosis. Sequence homologies indicate that the genome of the model plant *Arabidopsis thaliana* contains at least three open reading frames encoding presumptive Ap_4A hydrolases: At1g30110, At3g10620, and At5g06340. In this work we present efficient overexpression and detailed biochemical characteristics of the AtNUDX25 protein encoded by the At1g30110 gene. Aided by the determination of the binding constants of $Mn(Ap_4A)$ and $Mg(Ap_4A)$ complexes using isothermal titration calorimetry (ITC) we show that AtNUDX25 preferentially hydrolyzes Ap_4A in the form of a Mn^{2+} complex.

Keywords: Ap_4A hydrolase, Nudix, manganese, *Arabidopsis thaliana*

INTRODUCTION

Bis (5′-nucleosidyl) tetraphosphates are found in both eukaryotic and prokaryotic organisms at submicromolar concentrations (Garrison & Barnes, 1992; Guranowski, 2003). They were initially characterized as toxic side-products of protein synthesis, but more recently have been proposed to play a range of roles in processes such as control of DNA replication and repair, signaling in stress response, and apoptosis (for reviews see McLennan, 2000; 2006). Their *in vivo* concentration seems to be precisely controlled by a set of different enzymes including Ap_4A hydrolases (for reviews see Guranowski, 2000; 2004). Asymmetrical Ap_4A hydrolases [asymmetrical bis (5′-nucleosidyl) tetraphosphatases, EC 3.6.1.17] are enzymes which hydrolyse bis (5′-nucleosidyl) polyphosphates ($Np_{4-6}N'$) in such a way that a nucleosidyl triphosphate (NTP) is always one of the products. The favoured substrates of these enzymes are Ap_4A, Gp_4G and other bis (5′-nucleosidyl) tetraphosphates. Such enzymes have been identified in eukaryotes, among others in human and plants, and recently also in prokaryotes, including invasive bacteria (Warner & Finamore, 1965; Ogilvie & Antl, 1983; Jakubowski & Guranowski, 1983; Conyers & Bessman, 1999). The hydrolytic activity of asymmetrical Ap_4A hydrolases is based on a highly conserved sequence motif called the Nudix box ($Gx_5Ex_7REUxEExGU$, where x is any amino acid and U is a bulky hydrophobic residue) (Bessman *et al.*, 1996). A conserved

✉Corresponding author: Marta Dobrzańska, Institute of Biochemistry and Biophysics, A. Pawińskiego 5A, 02-106 Warszawa, Poland; tel.: (48) 22 592 1218; fax: (48) 22 658 4804; e-mail: martad@ibb.waw.pl

Abbreviations: Ap_3A, diadenosine 5′,5′′-P^1P^4 triphosphate; Ap_4A, diadenosine 5′,5′′-P^1P^4 tetraphosphate; Ap_5A, diadenosine 5′,5′′-P^1P^4 pentaphosphate; Ap_6A, diadenosine 5′,5′′-P^1P^4 hexaphosphate; DTT, dithiothreitol; FAD, flavin-adenine dinucleotide; Glu, glutamic acid; His, histidine; IPTG, isopropyl-β-D-thiogalactopyranoside; NAD, nicotinamide adenine dinucleotide; NADH, reduced form NAD^+; Nudix, nucleoside diphosphate linked to some other moiety x; 8-oxo-dGTP, 7, 8-dihydro-8-oxo-deoxyguanosine; Tyr, tyrosine.

Tyr residue located 16–18 amino acids downstream of the Nudix box is considered responsible for the preference of Ap_4A hydrolases for Ap_4A as their main substrate (Dunn *et al.,* 1999). Ap_4A hydrolases may be divided into two groups according to sequence homology. The plant and bacterial Ap_4A hydrolases have sequences similar to each other, but are substantially different from the human and animal ones. A comparison of structural data available for Ap_4A hydrolases from *Caenorhabditis elegans* and *Lupinus angustifolius* has shown that, despite of differences in protein sequences, these two proteins contain similar catalytic centers of three conserved glutamates in a spatial proximity (Swarbrick *et al.,* 2000; Maksel *et al.,* 2001; Bailey *et al.,* 2002). Two of these glutamates are within the Nudix motif and one is located elsewhere in the sequence.

A strict requirement for divalent metals to maintain their hydrolytic activity is a characteristic feature of all Nudix hydrolases (Mildvan *et al.,* 2005). In many cases more then one cation is needed to activate the enzyme. The precise roles of the metal ions in Nudix enzymes are not fully understood. It is proposed that one of the cations is bound to a conserved amino acid from the Nudix box, while the others may be bound to the oligophosphate substrate, orient the incoming nucleophile or neutralise the anionic leaving group (Mildvan *et al.,* 2005).

Since the announcement of its complete genome sequence, *Arabidopsis thaliana* has become an important model organism for plant molecular biology and genetics. Sequence homologies indicate that the *Arabidopsis thaliana* genome contains at least three open reading frames encoding presumptive Ap_4A hydrolases: At1g30110, At3g10620, and At5g06340. The protein products of two of these genes, At1g30110, At3g10620, have been obtained very recently as hexahistidine-tagged fusion proteins AtNUDX25 and AtNUDX26, respectively (Yoshimura *et al.,* 2007). Their activity toward different Nudix hydrolase substrates has been checked in the presence of 5 mM Mg^{2+} ions. Under such conditions the highest hydrolytic activity was observed for Ap_4A hydrolysis by AtNUDX25 but it was very low with the V_{max} of only 26.4 nmol min^{-1}mg $protein^{-1}$.

In this work we overexpressed of AtNUDX25 using pQE80 expression vector and performed a detailed biochemical characteristics of this protein with the main focus on its activation by different metal ions. Aided by the determination of the binding constants for the $Mn(Ap_4A)$ and $Mg(Ap_4A)$ complexes using isothermal titration calorimetry (ITC) we show that AtNUDX25 efficiently hydrolyzes Ap_4A in the form of a Mn^{2+} complex.

MATERIALS AND METHODS

Materials. The *A. thaliana* cDNA library was from Clontech. Oligonucleotide primers for polymerase chain reactions (PCR) were provided by the DNA Sequencing and Oligonucleotide Synthesis Service at the Institute of Biochemistry and Biophysics, Polish Academy of Sciences (Warszawa). Enzymes used in standard cloning reactions and *Taq* polymerase were from Fermentas. The pGEM-T Easy vector system I was supplied by Promega. The *Escherichia coli* expression vector pQE 80 and QIA-express kit type IV were from Qiagen. The *E. coli* strain Rosetta (DE3) was from Novagen. The complete EDTA-free protease inhibitor cocktail was from Roche Applied Science (Warszawa, Poland). All biochemicals and calf intestinal alkaline phosphatase were obtained from Sigma.

Cloning. The cDNA corresponding to the genomic sequence of At1g30110 was amplified from a commercial *A. thaliana* cDNA library with forward and reverse primers incorporating *Kpn*I and *Pst*I restriction sites, respectively. The PCR product was gel-purified and ligated into the pGEM-T Easy vector. The resulting plasmid was digested with *Kpn*I and *Pst*I, the insert was gel-purified, then ligated into the pQE80 vector and verified by sequencing. The resulting plasmid, pQE80At1g30110, with T7 lac promotor and a His-tag fusion upstream of the coding sequence was used to transform *E. coli* strain Rosetta (DE3) for expression.

Expression and purification of recombinant AtNUDX25 protein. A single colony was used to inoculate 10 ml of LB medium containing 100 μg/ml ampicillin and 24 μg/ml chloramphenicol. The culture was grown overnight at 37°C and 0.25 ml of the overnight culture was transferred to 50 ml of Luria–Bretani (LB) medium including the antibiotics, and grown to OD_{600} of 0.6. The expression was induced by adding IPTG to the final concentration of 0.5 mM, then the culture was incubated for additional 3 h. The cells were harvested by centrifugation, washed with an isotonic saline solution, resuspended in 1 ml of lysis bufer (0.5 M NaCl, 0.1 M Tris/HCl, pH 8.0, 5 mM β-mercaptoethanol plus 50 μl of the complete EDTA-free protease inhibitor cocktail), subjected to 4 or 5 freeze and thaw cycles (liquid N_2/room temp.), and centrifuged at 14 000 r.p.m. for 10 min at 4°C. The supernatant was then mixed with 0.25 ml of 50% nickel-nitrilotriacetic acid agarose (Qiagen). The recombinant protein was eluted with 250 mM imidazole, and dialysed overnight as described previously (Dobrzańska *et al.,* 2002). Unless indicated otherwise, either 5 mM β-mercaptoethanol or 1 mM DTT were used during the purification procedure.

Molecular mass determination. Electrospray ionization mass spectrometry (ESI-MS) was used to

determine the molecular mass of the recombinant protein. A sample of the protein was desalted using Vydac C18 HPLC column, then injected into a Q-Tof1 spectrometer (Micromass) at 4 μl/min, using a Hamilton syringe pump. Bovine pancreatic trypsin inhibitor was used as an internal mass standard. Positive ion spectra were deconvoluted using the MaxEnt 1 program (Waters Corp.).

Enzyme assay and kinetic studies. The progress of enzymatic reactions was followed either colorimetrically, at 800 nm, measuring inorganic phosphate liberated from the products of Ap_4A hydrolysis by calf intestine phosphatase (Ames & Dubin, 1960) or by ESI-MS in the negative ion mode, as described previously (Dobrzańska *et al.*, 2002). Briefly, the reaction mixture (20–50 μl) contained 50 mM Tris/HCl, pH 8.0, 3.5 mM $MnCl_2$, 1 mM DTT, variable Ap_4A concentrations ranging from 0.025 to 5.5 mM, 2–4 units of alkaline phosphatase, and 20 ng of the hydrolase. Reactions were stopped either by adding 280 μl of 10 mM EDTA or by heating at 95°C for 4 min. Calf intestine phosphatase was either omitted (negative ion spectra) or added after the reaction had been terminated by heating. In several cases Ap_4A (0.02 mM) the hydrolysis was followed spectrophotometrically. This general assay is based on an increase of A_{260} as a result of hydrolysis of dinucleoside polyphosphates (Jakubowski & Guranowski, 1983).

Isotermal titration calorimetry. The stability constants of Mn^{2+} and Mg^{2+} complexes of Ap_4A in 0.1 M Hepes buffer (pH 7.4), were measured at 25°C on a Microcal OMEGA ultrasensitive titration calorimeter (MicroCal Inc.). The solutions in the cell were stirred using a syringe at 400 r.p.m. Portions of the titrant (5 μl) were injected over 20 s with an interval of 240 s between injections from a 250 μl injection syringe into the sample cells (containing Ap_4A) in a series of several controlled pulses. The sample cell volume was 1.3611 cm^3. The integrated heat effects of each injection were corrected by subtraction of the corresponding integrated heat effects of $MnCl_2$ or $MgCl_2$ injection to pure buffer and the heat effects of buffer injection to the Ap_4A solution. Solutions of reactants were degassed prior to measurements. The Ap_4A concentration was determined by A_{260} absorbance, using the absorption coefficient ε_{260} = 27 100 $M^{-1} \cdot cm^{-1}$ (Holler *et al.*, 1983). The experimental data obtained from calorimetric titrations (five experiments done with two different sets of stock solutions) were analyzed assuming the model of a single set of identical sites (ITC Tutorial Guide).

RESULTS

Sequence analysis

The amino-acid sequences of all putative Ap_4A hydrolases encoded by the *A. thaliana* genomic sequences At1g30110, At3g10620, and At5g06340,

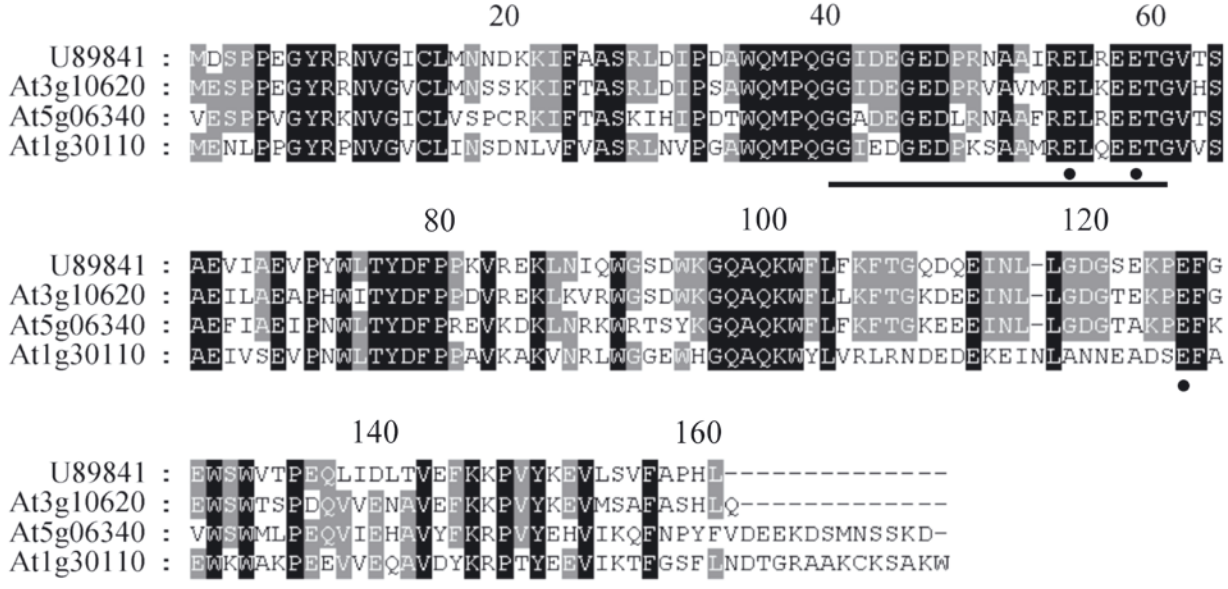

Figure 1. Sequence alignment of putative Ap_4A hydrolases from *Arabidopsis thaliana* encoded by genomic sequences At3g10620, At5g06340 and At1g30110 with the well-characterized Ap_4A hydrolase from *Lupinus angustifolius* L. (accession number U89841).

Residues strictly conserved among the four protein sequences are shaded black and those shared among three of the four sequences are shaded grey. The catalytic Nudix motif is underlined. The glutamate residues crucial for catalysis by lupin Ap_4A hydrolase are marked with black dots. The alignment was performed using MultiAlign program (INRA).

were compared using the Blast 2.0 program (National Center for Biotechnology Information, Bethesda, MD, USA) with the sequence of the best characterized plant Ap_4A hydrolase from *Lupinus angustifolius* L. (accession number U89841). The search revealed that all three sequences resembled the sequence of the lupin enzyme, with at least 53% of identical amino acids. All amino-acid residues shown to be crucial for the lupin Ap_4A hydrolase catalysis (Glu55, Glu59, Glu125) and specificity (Tyr77) were also conserved in the *A. thaliana* sequences (Maksel *et al*., 2001). A multialignment of the above proteins is presented in Fig. 1. The least similar of these protein sequences is that encoded by the At1g30110 gene and contains two unique blocks of amino-acid residues (aa 107–124 and 161–175) with no homology to the *L. angustifolius* Ap_4A hydrolase.

Expression and purification of recombinant Ap_4A hydrolase

The His_6-tagged At1g30110 gene product was expressed in *E. coli* transformed with the pQE80At1g30110 plasmid. Affinity chromatography on an immobilized-nickel column yielded a highly pure recombinant protein as revealed by SDS/PAGE (Fig. 2). The slightly higher than expected molecular mass of the major SDS/PAGE band (21.6 kDa) is typical for Nudix hydrolases, in particular for Ap_4A hydrolases, which migrate slowly during electrophoresis (Abdelghany *et al*., 2001).

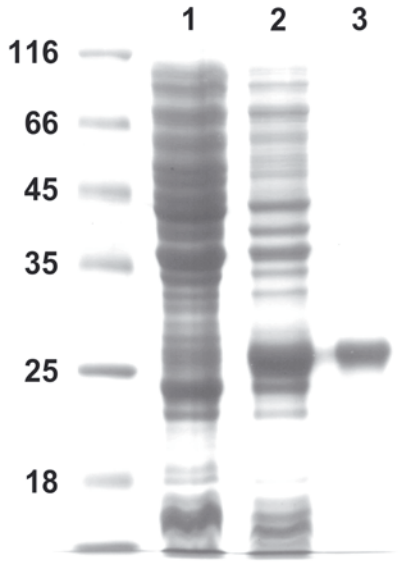

Figure 2. Expression and purification of recombinant hexahistidine-tagged *A. thaliana* protein encoded by the At1g30110 gene.
A Coomassie blue-stained SDS-12% gel shows: molecular mass standards (Fermentas), *E. coli* lysate with pQEAt1g30110 plasmid without induction (lane 1); *E. coli* lysate after 3 h induction with 0.5 mM IPTG (lane 2); and the His_6-tagged protein eluted from nickel affinity column with 250 mM imidazole (lane 3).

Electrospray ionization mass spectrometry (ESI-MS)

Mass spectrometry was used to precisely determine the molecular mass of the recombinant protein. A single peak with molecular mass of 21 671.25 ± 1.8 Da was observed. This mass is identical to the calculated mass of hexahistidine-tagged At1g30110 gene product (21 671.14 Da). In rare cases, we observed an additional peak at 21 823.50 ± 1.8 Da, corresponding to a mass increase of 152.25 Da. The peak disappeared after treating the sample with DTT and thus was assigned to the formation of a mixed disulfide with two 2-mercaptoethanol molecules per protein. Such samples were discarded.

Initial characterization of the recombinant protein in the presence of Mn^{2+} ions

Electrospray mass spectrometry of negative ions was applied for an initial characterization of the recombinant protein specificity. This method allows direct observation of the negatively charged substrates and products of the enzyme without a need to isolate them from the reaction mixture (Dobrzańska *et al*., 2002). Optimal conditions (buffer, pH and metal ion concentration) were searched for using a set of substrates including Ap_3A, Ap_4A, Ap_5A, Ap_6A, NADH, NAD, ADP-ribose, FAD, and 5-phosphoribosyl 1-pyrophosphate (PRPP) (Fisher *et al*., 2002). While almost no enzymatic activity was observed for any of these substrates in the presence of magnesium ions, products of Ap_4A hydrolysis, namely ATP and AMP, were clearly seen when manganese ions were used in the reaction mixture. A mass spectrum obtained for the hydrolysis of 2.0 mM Ap_4A in the presence of Mn^{2+} ions (3.5 mM) and 20 ng of AtNUDX25 at pH 8.0 is presented in Fig. 3. Among the other substrates tested only a slight cleavage of Ap_5A was observed, with ATP among the reaction products. In the presence of Mn^{2+} (3.5 mM) and Ap_4A (2.0 mM), the enzyme was active over a wide pH range, from 6.8 to 9.5, showing an optimum at around pH 8.0 (not shown). Relative activities of the enzyme towards Ap_4A, Ap_5A and Ap_6A were also measured using the colorimetric assay. This indirect test confirmed Ap_4A cleavage, and indicated enzymatic hydrolysis of Ap_5A and Ap_6A, at 10.4% and 6.5% of the rate of Ap_4A hydrolysis, respectively.

Activation of AtNUDX25 by divalent cations

The results presented in Table 1 summarize the data on activation of AtNUDX25 by various divalent cations as obtained by colorimetric experiments. These data confirm the preliminary MS observations

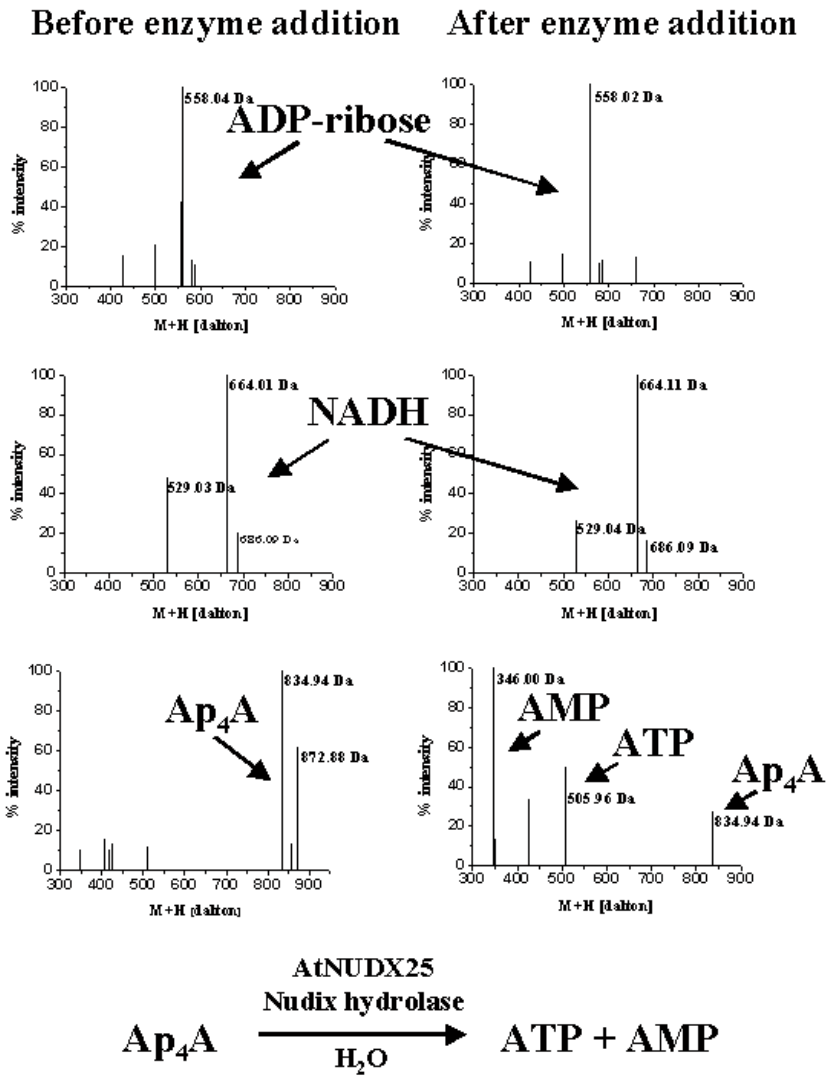

Figure 3. Substrate specificity of AtNUDX25 analyzed using negative-ion mass spectrometry.
Substrate solutions at 2 mM concentration were tested either before or after addition of the enzyme. The positions of standards are indicated.

that Mn^{2+} provides optimal activation for AtNUDX25. In the presence of Ap_4A (1.5 mM) no activity was seen with Mg^{2+}, Cd^{2+}, or Ca^{2+} at 1 mM concentrations, however, the enzyme exhibited a residual activity in the presence of Zn^{2+} ions. An increase of divalent cation concentrations to 5 mM resulted in weak enzyme activation for Cd^{2+}, Mg^{2+}, and Zn^{2+} ions (ordered by increasing activity); no activity was seen in the presence of Ca^{2+} ions. The enzyme was also inactive in the presence of 3.5 mM Mg^{2+} and two low Ap_4A concentrations, 0.1 and 0.02 mM (Table 1).

Stability constants of Ap_4A complexes

Varied stabilities of Ap_4A complexes with metal ions have been proposed in the literature. The constants provided previously by calorimetry (Tanner *et al.,* 2002) appear to be significantly overestimated, as discussed by Wszelaka-Rylik *et al.* (2007). A spectroscopic determination of the $Mn(Ap_4A)$ stability constant allows for the same conclusion (Conyers *et al.,* 2000). The conditional binding constant ${}^{c}K$ for the $Mn(Ap_4A)$ complex was determined here by ITC as $1.7 \pm 0.2 \times 10^4$ M^{-1}, corresponding to a dissociation constant $K_d = 59 \pm 8$ μM. The analogous constants for the $Mg(Ap_4A)$ complex, also determined here, were $5.5 \pm 0.2 \times 10^3$ M^{-1} and 183 ± 8 μM, respectively. The stabilities of these complexes are lower than those previously reported by Tanner *et al.* (2002) and Conyers *et al.* (2000).

Kinetic properties of the recombinant enzyme in the presence of Mn^{2+} ions

A series of experiments was performed to analyze in detail the influence of substrate and Mn^{2+}

Table 1. Effects of divalent metal ions (added as chlorides) on the activity of AtNUDX25 measured in the presence of Ap_4A.

All experiments were done using the colorimetric method except for measurements in the presence of 0.1 or 0.02 mM Ap_4A, which were followed spectrophotometrically.

Ap_4A concentration	Divalent metal ion concentration	Relative activity[a]
(mM)	(mM)	(%)
1.5	Mn^{2+}, 1.5	100.0
1.5	Mn^{2+}, 0.5	37.7
1.5	Ca^{2+}, 1.0	0
1.5	Ca^{2+}, 5.0	0
1.5	Zn^{2+}, 1.0	0.8
1.5	Zn^{2+}, 5.0	28.4
1.5	Mg^{2+}, 1.0	0
1.5	Mg^{2+}, 5.0	9.1
1.5	Cd^{2+}, 1.0	0
1.5	Cd^{2+}, 5.0	4.0
0.1	Mg^{2+}, 3.5	<0.2
0.02	Mg^{2+}, 3.5	<0.2

[a]Related to the rate of Ap_4A hydrolysis obtained in the reaction mixture containing 1.5 mM Ap_4A and 1.5 mM $MnCl_2$.

concentration on AtNUDX25 enzyme properties. The concentrations of the Ap_4A hydrolysis products, ATP and AMP, were estimated after terminating the enzymatic reaction by heating, using indirect colorimetric assays which measure the concentration of phosphate released from these mononucleotides by alkaline phosphatase. In some experiments the phosphatase was added during the enzymatic reaction to avoid the hypothetical product inhibition of AtNUDX25. The presence of alkaline phosphatase did not affect the rates of the catalyzed reaction. The dependence of the rate of hydrolysis on Mn^{2+} at the constant Ap_4A concentration of 1 mM (expressed as inverse logarithm of the total Mn^{2+} concentration, pMn) is presented in Fig. 4. The initial concentrations of the $Mn(Ap_4A)$ complex and of free Ap_4A in these enzymatic reactions are also plotted. These concentrations were calculated from the binding constant determined above here. The curve generated by plotting the rate of Ap_4A hydrolysis as a function of pMn has two sigmoidal sectors of opposite inclinations. The optimal enzyme activity range is very narrow. The maximal activity of the enzyme in this series of experiments, 27.0 ± 1.0 μmol/min per mg, coincided with total Mn^{2+} and Ap_4A concentrations of 1 mM. At such concentrations the $Mn(Ap_4A)$ complex dominates and the concentration of its components (denoted by square brackets) $[Mn^{2+}] = [Ap_4A] = 83$ μM. An excess of either $[Mn^{2+}]$ or $[Ap_4A]$ over $[Mn(Ap_4A)]$ results in a decrease of the reaction rate. The fits of the sigmoidal sectors of the pMn curve to the Hill equation (Hill, 1910; Acerenza & Mizraji, 1997) yielded apparent K_d values of 195 ± 13 μM with $n_1 = 2.0 \pm 0.2$ for the low Mn^{2+} branch and of 1.82 ± 0.12 mM with $n_2 = 2.9 \pm 0.8$ for the high Mn^{2+} branch (n_1 and n_2 are respective Hill coefficients). The n_1 value indicates that at least two Mn^{2+} binding sites must be occupied to activate the enzyme. The value of n_2 was determined with a much lower accuracy, not allowing firm conclusion about the stoichiometry of the manganese-related inhibition.

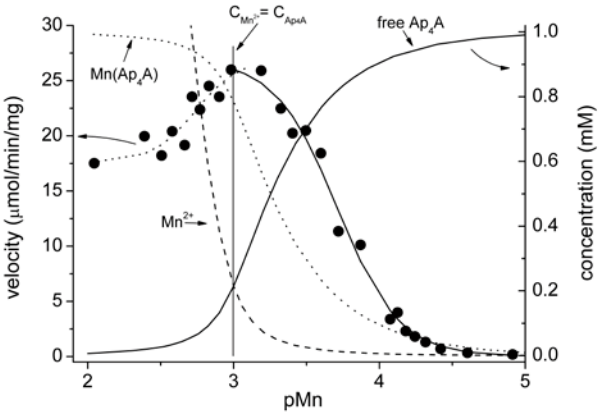

Figure 4. AtNUDX25 activity at total Ap_4A concentration of 1 mM, as a function of Mn^{2+} ion concentration, along with the fit to the Hill equation (-).
Initial concentrations of $Mn(Ap_4A)$, free Mn^{2+}, and free Ap_4A are shown for comparison. The activity was determined colorimetrically at 800 nm (Ames & Dubin, 1960).

Curves generated by plotting the velocities of Ap_4A hydrolysis by AtNUDX25 as a function of to-

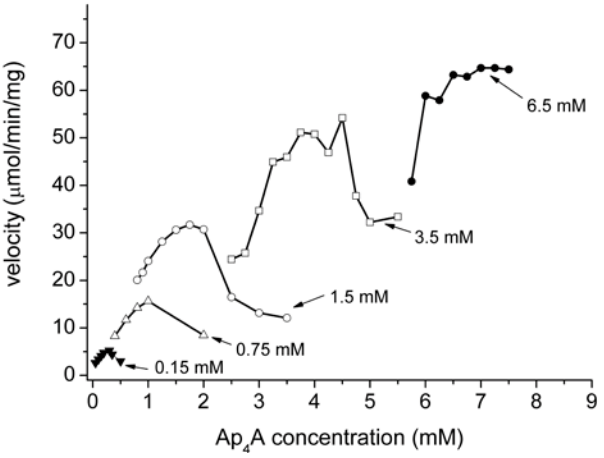

Figure 5. AtNUDX25 activity as a function of total Ap_4A concentration.
The data are means of triplicate assays. The data points outside the maxima, as well as the standard errors of the mean (typically within 4% of the respective values) are omitted for clarity. The total concentrations of $MnCl_2$ in individual curves are indicated. The activity was determined colorimetrically at 800 nm (Ames & Dubin, 1960).

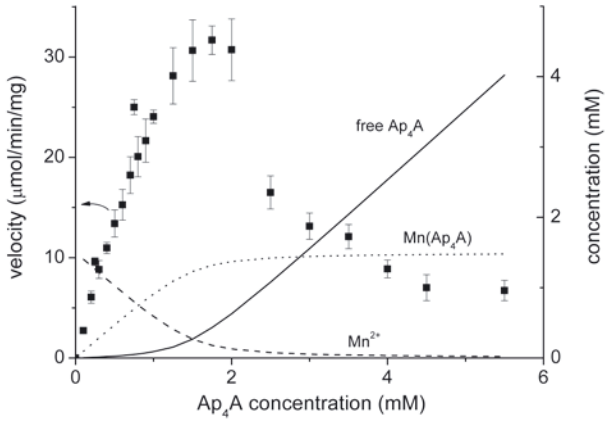

Figure 6. AtNUDX25 activity as a function of Ap_4A concentration, at the $MnCl_2$ concentration of 1.5 mM, compared with initial concentrations of $Mn(Ap_4A)$, free Mn^{2+} and free Ap_4A.
The activity was determined colorimetrically at 800 nm (Ames & Dubin, 1960).

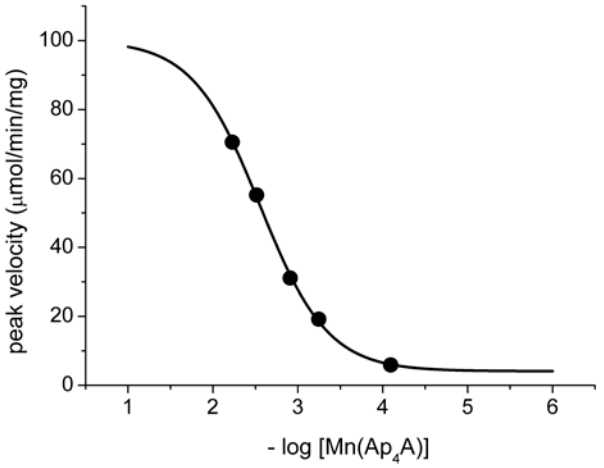

Figure 7. Peak AtNUDX25 activities as a function of $Mn(Ap_4A)$ concentrations, along with the fit to the Hill equation (–).

tal Ap_4A concentration, determined at several Mn^{2+} concentrations, are presented in Fig. 5. At each of the Mn^{2+} concentrations tested, 0.15, 0.75, 1.5, 3.5, and 6.5 mM, the AtNUDX25 activity as a function of $[Ap_4A]$ increased up to the point of maximal activation, 5.9, 19.2, 31.1, 55.2, and 70.5 μmol/min per mg, respectively, and then decreased. To elucidate this effect, the initial values of $[Mn^{2+}]$, $[Ap_4A]$ and $[Mn(Ap_4A)]$ were calculated for these experiments. Fig. 6 presents comparisons of these concentrations with the hydrolysis rates for a total Mn^{2+} concentration of 1.5 mM. The point of maximal activation of the enzyme coincided with equimolar Mn^{2+} and Ap_4A for all concentrations tested.

The dependence of V_{max} of Ap_4A hydrolysis by AtNUDX25 on log concentrations of $Mn(Ap_4A)$ is presented in Fig. 7. The fitting of this sigmoidal relationship to the Hill equation yielded K_d of 2.5 ± 1 mM, and the corresponding Hill coefficient $n_3 = 0.94 \pm 0.17$. Extrapolations of V_{max} values to high and low complex concentrations yielded the limiting maximal and minimal velocities of 104 ± 18 and 4.4 ± 2 μmol/min per mg, respectively.

DISCUSSION

Asymmetrical Ap_4A hydrolases are suggested to be key enzymes participating in the regulation of intracellular concentration of Ap_4A, and to a smaller extent, of other adenosine polyphosphates (Guranowski, 2000). Despite their importance in many organisms, no efficient Ap_4A hydrolases have been characterized so far in the model plant — *A. thaliana*. At1g30110 is one of the three genomic sequences from *A. thaliana* proposed to encode an Ap_4A hydrolase. The full-length At1g30110 gene, including six introns, comprises 1940 bp, and the open reading frame encodes a 175-amino-acid protein with a deduced molecular mass of 21 671.14 Da and pI 4.8. We have developed an efficient method for bacterial overexpression of the AtNUDX25 protein using pQE 80 expression system. The recombinant protein is capable of efficiently degrading Ap_4A in the cleavage pattern typical for Ap_4A hydrolases (Lobatón *et al.*, 1975; Jakubowski & Guranowski, 1983). The alkaline pH optimum of the enzyme is typical for asymmetrically acting Ap_4A hydrolases. Under the conditions used in this study none of other standard Nudix hydrolase substrates, such as Ap_3A, NADH, NAD, ADP-ribose, PRPP and FAD, was hydrolysed by AtNUDX25. A notable difference between this enzyme and the plant hydrolase studied earlier is in the hydrolysis of substrates with more than four phosphate groups. AtNUDX25 digested Ap_5A and Ap_6A much more slowly than did the other plant Ap_4A hydrolase (Jakubowski & Guranowski, 1983). The rates of Ap_5A and Ap_6A hydrolysis were only 10.4% and 6.5% of the rate of Ap_4A hydrolysis, in comparison to 42% and 34%, respectively, reported for the lupin enzyme (Jakubowski & Guranowski, 1983). In this regard AtNUDX25 resembles the *Caenorhabditis elegans* Ap_4A hydrolase (Abdelghany *et al.*, 2001).

The presence of metal ions, often more than one per enzyme molecule, is a prerequisite for activation of all Nudix enzymes, but the number and type of the cations needed for efficient catalysis varies depending on the subtype of the hydrolases (for a review see Mildvan *et al.*, 2005). In most cases, Mg^{2+} ions have been shown to be preferred by eukaryotic Ap_4A hydrolases (Guranowski *et al.*, 2000). Several of these hydrolases, although preferentially activated by Mg^{2+} ions, were shown to maintain

their activity in the sole presence of Mn^{2+} ions (Jakubowski & Guranowski, 1983). Recently, very inefficient Ap_4A hydrolysis was detected by others for AtNUDX25 in the presence of 5 mM magnesium ion (Yoshimura *et al*., 2007). Table 1 presents the effect of different divalent cations on the Ap_4A hydrolysis by AtNUDX25. The strong preference of AtNUDX25 for Mn^{2+} ions is remarkable. We were unable to observe any hydrolysis of 1.5 mM Ap_4A in the presence of Ca^{2+}. The enzyme required high (5 mM) Mg^{2+}, Cd^{2+}, and Zn^{2+} concentrations to cleave some substrate (<10%), but never reached the activity provided by Mn^{2+} ions. Since the human Mg^{2+}-dependent Ap_4A hydrolase was strongly inhibited when substrate concentrations exceeded 10 μM (Hankin *et al*., 1995), we additionally tested the activity of AtNUDX25 in the presence of 3.5 mM Mg^{2+} and two low Ap_4A concentrations, 0.1 and 0.02 mM, using a more sensitive spectrophotometric assay (Jakubowski & Guranowski, 1983). In both cases we failed to detect even a trace of Ap_4A hydrolysis. Therefore we can state that Mn^{2+}, and not Mg^{2+}, is a true activator of AtNUDX25. Recently, an enzyme from *Deinococcus radiodurans* was characterized which showed a strong Mn^{2+} dependence of Ap_nA hydrolysis, with Mg^{2+} ions at 15 mM giving only 5% of the activity accomplished by 2 mM Mn^{2+} (Fisher *et al*., 2006).

The involvement and number of Mn^{2+} ions participating in Ap_4A hydrolysis was studied earlier for the hydrolase from *Bartonella bacilliformis*, which required three Mn^{2+} ions. One of them was proposed to be substrate-bound (Conyers *et al*., 2000). Similarly, two Mn^{2+} ions were found to activate another Nudix hydrolase, 8-oxo-dGTPase (MutT) (Frick *et al*., 1994). The kinetic data presented above indicated that at least two Mn^{2+} ions participated cooperatively in the AtNUDX25-catalyzed reaction, when [Ap_4A] was in excess over [Mn^{2+}] (Fig. 4). This view is supported both by the Hill coefficient value $n_1 = 2.0$, and by an absence of systematic deviations of the fit. Interestingly, the maximum of enzymatic activity, regardless of the concentration of Ap_4A and Mn^{2+}, always coincided with their equimolarity (Figs. 4–6), indicating that one Mn^{2+} ion interacted with Ap_4A directly. It is generally known that enzymes involved in the hydrolysis of oligophosphates prefer as true substrates their complexes with M^{2+} rather than free ligands (Toscano *et al*., 2003). For AtNUDX25 this view is confirmed by the analysis presented in Fig. 7, which shows that the maximum activity of the enzyme, measured at equimolar Ap_4A and Mn^{2+}, depends directly on the concentration of the Mn(Ap_4A) complex. The value of $n_3 = 0.94 \pm 0.17$ for the fitted Hill curve indicates a simple, non-cooperative interaction. The dissociation constant for the Mn(Ap_4A) complex interaction with the enzyme, provided by this calculation, is 2.5 ± 1 mM. This value is somewhat underestimated, due to an inhibition by free Ap_4A and free Mn^{2+}, always present as a result of the relatively low stability of the Mn(Ap_4A) complex (see Figs. 4 and 6). A semi-quantitative analysis of the inhibitory branches of the kinetic curves at high Ap_4A, presented in Figs. 5 and 6 suggests, however, that the error in peak velocity determinations, introduced by this effect, is small, approx. 3–5%. The V_{max} value for Mn(Ap_4A) as substrate, determined from the fit, was 104 ± 18 μmol/min per mg.

These facts suggest a situation akin to that found for the *Bartonella bacilliformis* Ap_4A hydrolase and MutT, where the Mn(Ap_4A) and Mn(8-oxo-dGTP) complexes, respectively, were proposed to be true substrates for these enzymes, while the remaining Mn^{2+} ion(s) interacted directly with the protein residues (Frick *et al*., 1994; Conyers *et al*., 2000). The latter view is also supported by the selectivity of AtNUDX25 activation, which is certainly due to the protein-based metal binding site(s). The formation of the Mn(Ap_4A) complex may not be responsible for the selectivity of AtNUDX25 activation. Ap_4A alone is not so strongly selective for Mn^{2+}, as indicated by the similar stabilities of its Mn^{2+}, Mg^{2+}, and Zn^{2+} complexes: K_d values of 59, 183, and 138 μM, respectively; the latter value was recalculated from published data (Wszelaka-Rylik *et al*., 2007). One has to note that our protein contains a hexahistidine affinity tag, which might provide a binding site for Mn^{2+} ions. The chemistry of such interactions has not been reported, but a study of Ni^{2+} interactions with the His-tag suggests that a corresponding interaction with Mn^{2+} ions would not be effective (Valenti *et al*., 2006).

A series of Ap_4A titrations at fixed Mn^{2+} levels demonstrated that an excess of Ap_4A concentration over Mn^{2+} concentration resulted in a partial inhibition of the AtNUDX25 activity (Figs. 5 and 6). The overall profiles of such Ap_4A titrations were analogous to the profile of Mn^{2+} titration presented in Fig. 4, but the branches of these curves could not be fitted to the Hill equation (Acerenza & Mizraji, 1997). This complex behavior seems to be due to overlapping effects of the cooperativity between Ap_4A and Mn^{2+}, to form free and enzyme-bound Mn(Ap_4A) complexes, and of the competition between Ap_4A and AtNUDX25 for Mn^{2+} ions. Moreover, at low Ap_4A concentrations AtNUDX25 may be activated by Ap_4A, because it will first remove the inhibitory excess of Mn^{2+} ions.

We have previously reported that another Nudix protein, AtNUDX1, is active toward NADH in the presence of 5 mM Mn^{2+} (Dobrzańska *et al*., 2002). Later, Klaus *et al*. (2004) reported that the activity fell drastically as Mn^{2+} concentration approached the usual 5 μM physiological range, and

at that concentration the enzyme activity was only 0.001% of that found at 5 mM. An extrapolation of AtNUDX25 activity from millimolar to micromolar concentrations may be attempted by comparing the saturation of Ap_4A by Mn^{2+} at these two concentration ranges. This leads to an extrapolated activity of ATNUDX25 at 5 μM substrate as low as 0.025% of that interpolated for 5 mM, thus about 0.017 μmol/min/mg. The same reason may be responsible for the behavior of AtNUDX1. Of course, this extrapolation is very tentative, due to the complicated and only partially elucidated character of AtNUDX25 inhibition by free Ap_4A.

Our experiments characterised the AtNUDX25 protein as an atypical eukaryotic Ap_4A hydrolase, which is most selectively activated by manganese ions. In general, the complicated character of the catalytic process of Nudix, and in particular of Ap_4A hydrolases (Mildvan *et al.*, 2005), makes predictions of their *in vivo* role very speculative, especially as neither the presence nor the level of Ap_4A in plant cells have ever been reported. Low levels (0.05–5 μM) of various oligophosphates, including Ap_4A, have been shown to exist in other eukaryotic cells (Garrison & Barnes, 1992). The intracellular concentration of Mn^{2+} is in the micromolar range (Schinkmann & Blenis, 1997). When the intracellular Mn^{2+} and Ap_4A concentrations in eukaryotic organisms are taken into account, the catalytic power of AtNUDX25 must be low, as estimated above. However, it might be important that AtNUDX25 hydrolyzes Ap_4A when its concentration approaches the concentration of Mn^{2+} ions. We can therefore speculate that the protein acts in signal transduction to record intracellular manganese concentration with respect to Ap_4A or contrariwise in the case of spikes of their concentrations. Proteins behaving in such a fashion are known to respond to Ca^{2+} spikes (Berridge *et al.*, 2003).

Acknowledgements

This work was supported by the State Committee for Scientific Research Grant no. PBZ-KBN-110/P04/2004.

We would like to thank Jacek Olędzki for excellent technical assistance in mass analysis and Arkadiusz Ciesielski for help in figure preparation. We are grateful to Professor Grażyna Muszyńska and Professor Jan Miernyk for helpful comments and suggestions.

REFERENCES

Abdelghany HM, Gasmi L, Cartwright JL, Bailey S, Rafferty JB, McLennan AG (2001) Cloning, characterisation and crystallisation of a diadenosine 5′,5‴-P(1),P(4)-tetraphosphate pyrophosphohydrolase from *Caenorhabditis elegans*. *Biochim Biophys Acta* **1550**: 27–36.

Acerenza L, Mizraji E (1997) Cooperativity: a unified view. *Biochim Biophys Acta* **1339**: 155–166.

Ames BN, Dubin DT (1960) The role of polyamines in the neutralization of bacteriophage deoxyribonucleic acid. *J Biol Chem* **235**: 769–775.

Bailey S, Sedelnikova SE, Blackburn GM, Abdelghany HM, Baker PJ, McLennan AG, Rafferty JB (2002) The crystal structure of diadenosine tetraphosphate hydrolase from *Caenorhabditis elegans* in free and binary complex forms. *Structure* **10**: 589–600.

Berridge MJ, Bootman MD, Roderick HL (2003) Calcium signalling: dynamics, homeostasis and remodelling. *Nat Rev Mol Cell Biol* **4**: 517–529.

Bessman MJ, Frick DN, O`Handley SF (1996) The MutT proteins or "Nudix" hydrolases, a family of versatile, widely distributed "housecleaning" enzymes. *J Biol Chem* **271**: 25059–25062.

Conyers GB, Bessman MJ (1999) The gene, ialA, associated with the invasion of human erythrocytes by *Bartonella bacilliformis*, designates a nudix hydrolase active on dinucleoside 5′-polyphosphates *J Biol Chem* **274**: 1203–1206.

Conyers GB, Wu G, Bessman MJ, Mildvan AS (2000) Metal requirements of a diadenosine pyrophosphatase from *Bartonella bacilliformis*: magnetic resonance and kinetic studies of the role of Mn^{2+}. *Biochemistry* **39**: 2347–2354.

Dobrzańska M, Szurmak B, Wysłouch-Cieszyńska A, Kraszewska E (2002) Cloning and characterization of the first member of the Nudix family from *Arabidopsis thaliana*. *J Biol Chem* **277**: 50482–50486.

Dunn CA, O'Handley SF, Frick DN, Bessmann MJ (1999) Studies on the ADP-ribose pyrophosphatase subfamily of the Nudix hydrolases and tentative identification of *trgB*, a gene associated with tellurite resistance. *J Biol Chem* **274**: 32318–33324.

Garrison PN, Barnes LD (1992) Determination of dinucleoside polyphosphates. In *Ap_4A and Other Dinucleoside Polyphosphates.* McLennan AG ed, pp 29–61. CRC Press, Boca Raton, FL

Fisher DI, Safrany ST, Strike P, Mc Lennan AG (2002) Nudix hydrolases that degrade dinucleoside and diphosphoinositol polyphosphates also have 5-phosphoribosyl 1-pyrophosphate (PRPP) pyrophosphatase activity that generates the glycolytic activator ribose 1,5-bisphosphate. *J Biol Chem* **47**: 47313–47317.

Fisher DI, Cartwright IL, McLennan AG (2006) Characterization of the Mn^{2+}-stimulated (di)adenosine polyphosphate hydrolase encoded by the *Deinococcus radiodurans* DR2356 nudix gene. *Arch Microbiol* **180**: 415–424.

Frick DN, Weber DJ, Gillespie JR, Bessman MJ, Mildvan AS (1994) Dual divalent cation requirement of the MutT dGTPase. Kinetic and magnetic resonance studies of the metal and substrate complexes. *J Biol Chem* **269**: 1794–1803.

Guranowski A (2000) Specific and nonspecific enzymes involved in the catabolism of mononucleoside and dinucleoside polyphosphates. *Pharmacol Ther* **87**: 117–139.

Guranowski A (2003) Analogs of diadenosine tetraphosphate (Ap_4A). *Acta Biochim Polon* **50**: 947–972.

Guranowski A (2004) Metabolism of diadenosine tetraphosphate (Ap_4A) and related nucleotides in plants; review with historical and general perspective**.** *Front Biosci* **1**: 1398–1341.

Hankin S, Thorne NMH, McLennan AG (1995) Diadenosine 5′,5″-P^1,P^4-tetraphosphate hydrolase is present in human erythrocytes, leukocytes and platelets. *Int J Biochem Cell Biol* **27**: 201–206.

Hill AV (1910) The possible effects of the aggregation of the molecules of haemoglobin on its dissociation curves. *J Physiol* (London) **40**: 4–7.

Holler E, Holmquist B, Vallee B, Taneja K, Zamecnik P (1983) Circular dichroism and ordered structure of bisnucleoside oligophosphates and their Zn^{2+} and Mg^{2+} complexes. *Biochemistry* **22**: 4924–4933.

Jakubowski H, Guranowski A (1983) Enzymes hydrolyzing ApppA and/or AppppA in higher plants. Purification and some properties of diadenosine triphosphatase, diadenosine tetraphosphatase, and phosphodiesterase from yellow lupin (*Lupinus luteus*) seeds. *J Biol Chem* **258**: 9982–9989.

Klaus SM, Wegkamp A, Sybesma W, Hugenholtz J, Gregory JF 3rd, Hanson A (2004) A nudix enzyme removes pyrophosphate from dihydroneopterin triphosphate in the folate synthesis pathway of bacteria and plants. *J Biol Chem* **280**: 5274–5280.

Lobatón CD, Vallejo CG, Sillero A, Sillero MA (1975) Diguanosinetetraphosphatase from rat liver: Activity on diadenosine tetraphosphate and inhibition by adenosine tetraphosphate. *Eur J Biochem* **50**: 495–501.

Maksel D, Gooley PR, Swarbrick JD, Guranowski A, Gange C, Blackburn GM, Gayer KR (2001) Characterization of active-site residues in diadenosine tetraphosphate hydrolase from *Lupinus angustifolius*. *Biochem J* **357**: 399–405.

McLennan AG (2000) Dinucleoside polyphosphates-friend or foe? *Pharmacol Ther* **87**: 73–89.

McLennan AG (2006) The Nudix hydrolase superfamily. *Cell Mol Life Sci* **63**: 123–143.

Mildvan AS, Xia Z, Azurmendi HF, Saraswat V, Legler PM, Massiah MA, Gabelli SB, Bianchet MA, Kang L-W, Amzel LM (2005) Structures and mechanisms of Nudix hydrolases. *Arch Biochem Biophys* **433**: 129–143.

Ogilvie A, Antl W (1983) Diadenosine tetraphosphatase from human leukemia cells. Purification to homogeneity and partial characterization. *J Biol Chem*. **258**: 4105–4109.

Schinkmann K, Blenis J (1997) Cloning and characterization of a human STE20-like protein kinase with unusual cofactor requirements. *J Biol Chem* **272**: 28695–28703.

Swarbrick JD, Bashtannyk T, Maksel D, Zhang XR, Blackburn GM, Gayler KR, Gooley PR (2000) The three-dimensional structure of the Nudix enzyme diadenosine tetraphosphate hydrolase from *Lupinus angustifolius* L. *J Mol Biol* **302**: 1165–1177.

Swarbrick JD, Buyya S, Gunawardana D, Gayler KR, McLennan AG, Gooley PR (2005) Structure and substrate-binding mechanism of human Ap_4A hydrolase. *J Biol Chem* **280**: 8471–8481.

Tanner JA, Abowath A, Miller AD (2002) Isothermal titration calorimetry reveals a zinc ion as an atomic switch in the diadenosine polyphosphates. *J Biol Chem* **277**: 3073–3078.

Toscano WA, Toscano JS, Toscano DG, Gross MK (2003) Molecular modeling of manganese regulation of calmodulin-sensitive adenylyl cyclase from mammalian sperm. *Biochem Biophys Res Commun* **312**: 91–96.

Valenti LE, De Pauli CP, Giacomelli CE (2006) The binding of Ni(II) ions to hexahistidine as a model system of the interaction between nickel and His-tagged proteins. *J Inorg Biochem* **100**: 192–200.

Warner AH, Finamore FJ (1965) Isolation, purification, and characterization of P1,P4–diguanosine 5′-tetraphosphate asymmetrical-pyrophosphohydrolase from brine shrimp eggs. *Biochemistry* **4**: 1568–1575.

Wszelaka-Rylik M, Witkiewicz-Kucharczyk A, Wójcik J, Bal W (2007) Ap_4A is not an efficient Zn(II) binding agent. A concerted potentiometric, calorimetric and NMR study. *J Inorg Biochem* **101**: 758–763.

Yoshimura K, Ogawa T, Ueda Y, Shigeoka S (2007) *AtNUDX1*, an 8-oxo-7,8-dihydro-2′-deoxyguanosine 5′-triphosphate pyrophosphohydrolase, is responsible for eliminating oxidized nucleotides in *Arabidopsis*. *Plant Cell Physiol* **48**: 1438–1449.